

The Lyman- α emission of high- z damped Lyman- α systems

H. Rahmani^{1*}, R. Srianand¹, P. Noterdaeme² & P. Petitjean³

¹ *Inter-University Centre for Astronomy and Astrophysics, Post Bag 4, Ganeshkhind, Pune 411 007, India*

² *Departamento de Astronomía, Universidad de Chile, Casilla 36-D, Las Condes, Santiago, Chile*

³ *Université Paris 6, UMR 7095, Institut d'Astrophysique de Paris-CNRS, 98bis Boulevard Arago, 75014 Paris, France*

Accepted. Received; in original form

ABSTRACT

Using a spectral stacking technique we searched for the average Ly α emission from high- z Damped Ly α (DLA) galaxies detected in the Sloan Digital Sky Survey QSO spectra. We used a sample of 341 DLAs of mean redshift $\langle z \rangle = 2.86$ and $\log N(\text{H I}) \geq 20.62$ to place a 3σ upper limit of $3.0 \times 10^{-18} \text{ erg s}^{-1} \text{ cm}^{-2}$ on the Ly α flux emitted within ~ 1.5 arcsec (or 12 kpc) from the QSO line of sight. This corresponds to an average Ly α luminosity of $\leq 2 \times 10^{41} \text{ erg s}^{-1}$ or $0.03 L_*(\text{Ly}\alpha)$. This limit is deeper than the limit of most surveys for faint Ly α emitters. The lack of Ly α emission in DLAs is consistent with the in situ star formation, for a given $N(\text{H I})$, being less efficient than what is seen in local galaxies. Thus, the overall DLA population seems to originate from the low luminosity end of the high redshift Ly α emitting galaxies and/or to be located far away from the star forming regions. The latter may well be true since we detect strong O VI absorption in the stacked spectrum, indicating that DLAs are associated with a highly ionized phase possibly the relics of galactic winds and/or originating from cold accretion flows. We find the contribution of DLA galaxies to the global star formation rate density to be comparatively lower than that of Lyman Break Galaxies.

Key words: galaxies: quasar: absorption line – galaxies: intergalactic medium

1 INTRODUCTION

Damped Ly α (DLA) systems, detected in absorption in the spectra of background quasars are characterized by large neutral hydrogen column densities ($N(\text{H I}) \geq 2 \times 10^{20} \text{ cm}^{-2}$) and represent the main reservoir of H I at high- z (see Noterdaeme et al. 2009, Fig. 14). The presence of associated heavy elements, the evolution with redshift of the mass density in DLAs, a signature of gas consumption via star formation and the detectability of DLAs over a wide range of redshift make them the appropriate laboratories for studying the cosmological evolution of star formation activity in a luminosity unbiased way.

Though observational studies of DLAs have been pursued over 25 years, one of the most important questions that remain unanswered yet is the connection between DLAs and star-forming galaxies. Measuring the star formation rate (SFR) in DLA-galaxies is very important as DLAs could provide substantial contributions to the global SFR density at high redshifts (Wolfe et al. 2003b; Srianand et al. 2005).

At low and intermediate redshifts ($z < 1$), galaxy counterparts of DLAs have been identified in a number of cases (Burbidge et al. 1996; Le Brun et al. 1997; Rao et al. 2003). They are usually low surface brightness dwarf galaxies (see Rao et al. 2003). On the other hand, searches for the direct emission of the

high redshift (i.e. $z > 1$) DLA galaxies have resulted in a number of non-detections (Lowenthal et al. 1995; Bunker et al. 1999; Colbert & Malkan 2002; Kulkarni et al. 2006; Christensen et al. 2007) and only a few cases have been spectroscopically confirmed through detection of Ly α emission (Warren & Moller 1996; Moller et al. 1998; Møller et al. 2002, 2004; Heinmüller et al. 2006; Fynbo et al. 2010). The difficulty is mainly attributed to the faint nature of the DLA galaxies and their apparent closeness to the bright background QSOs.

One indirect way to address this question is to study the relative populations of different rotational levels of molecular hydrogen (H_2) together with that of fine-structure levels of C I and C II. The ambient UV flux and therefore the in-situ SFR can thus been derived (e.g. Hirashita & Ferrara 2005; Srianand et al. 2005; Noterdaeme et al. 2007) in a few of the $\sim 10\%$ of DLAs that show detectable amounts of H_2 (Petitjean et al. 2000; Ledoux et al. 2003; Noterdaeme et al. 2008). The rotational excitation seen in these H_2 bearing DLAs is consistent with an ambient UV radiation field similar to or higher than the Galactic one (Srianand et al. 2005). This may not be representative of the overall population however.

Another indirect approach is to derive the SFR through the cooling rate inferred from the C II $\lambda 1335$ absorption lines as suggested by Wolfe et al. (2003a). They have estimated an average SFR per unit area of $10^{-2.2} M_\odot \text{ yr}^{-1} \text{ kpc}^{-2}$ or $10^{-1.3} M_\odot \text{ yr}^{-1} \text{ kpc}^{-2}$ if DLAs arise in cold neutral medium (CNM) or warm neutral medium (WNM) respectively. However, appreciable contribution

* E-mail: hadi@iucaa.ernet.in

of C II π absorption from the warm ionised medium (WIM) as observed in the diffuse gas of the Milky Way (Lehner et al. 2004) will make the inferred SFR based on C II π absorption lines unreliable.

Thanks to the availability of a very large number of moderate resolution QSO spectra in the SDSS data base, it is possible to directly detect emission from the galaxy counterparts within 1.5 arc sec to the line of sight (Noterdaeme et al. 2010) and/or to measure the average SFR in different types of QSO absorption systems by detecting nebular emission in the stacked spectra (Wild et al. 2007; Noterdaeme et al. 2010; Ménard et al. 2009). Here, we tried to measure the average Ly α emission from DLAs using spectral stacking techniques. We describe our DLA sample in Section 2, discuss the stacking technique we use and the results in Section 3. We discuss the O VI detections in Section 5 and contribution of DLAs to global SFR density in Section 4. Our conclusions are presented in Section 6. Throughout this paper we assume a standard flat Λ CDM universe with $H_0 = 71 \text{ km s}^{-1} \text{ Mpc}^{-1}$, $\Omega_M = 0.26$, $\Omega_\Lambda = 0.74$.

2 DLA SAMPLE

The sample of DLAs used here mainly comes from an automatic search for DLAs in the Sloan Digital Sky Survey II, Data Release 7 (Noterdaeme et al. 2009). This sample contains 1426 absorbers at $2.15 < z < 5.2$ with $\log N(\text{H I}) \geq 20$, out of which 937 systems have $\log N(\text{H I}) \geq 20.3$. We also use additional DLAs found by Prochaska & Wolfe (2009). In total, there are 914 DLAs with redshift measurements based on metal absorption lines. We notice that the poor background subtraction leaves some spikes in the locations of strong sky lines. To avoid any systematics due to these features we have excluded systems located in regions of strong sky lines¹.

In order to establish the presence or absence of any Ly α emission, we need the bottom of the DLA absorption profile to be defined by enough pixels with zero flux. We will use only those DLAs for which the core (with zero flux) extends over at least three FWHM elements. Since the spectral resolution of SDSS spectra is about $R = 2000$, the rest FWHM of an unresolved Ly α emission is $\sim 0.61 \text{ \AA}$. The above condition translates to a lower limit on the H I column density of $\log N(\text{H I}) = 20.62$.

By visual inspections of the individual spectra, we rejected systems showing a double absorption feature in either their Ly β or metal absorption profiles. Indeed some of these systems may not be real DLAs as the high Ly α equivalent width may be the result of the blend of several components. We also rejected proximate DLAs located within 5000 km s^{-1} from the QSO redshift and ensured that there is no contamination of the sample by broad absorption lines. After applying all these conditions we are left with 341 systems with $\log N(\text{H I}) \geq 20.62$ that forms our sample to be used in the stacking exercise.

3 SPECTRAL STACKING

The observed SDSS spectra were first shifted to the rest frame of the DLA conserving the flux per unit wavelength interval. The residual flux level in the core of the DLA absorption profile generally shows some non-zero off-set probably related to sky subtraction errors. We correct this off-set using the median flux in the

Table 1. Ly α measurement in the stacked spectrum.

Stacking method	$F(\text{Ly}\alpha)^a$	$F_{3\sigma}(\text{Ly}\alpha)^b$	$L_{3\sigma}(\text{Ly}\alpha)^b$
simple mean	0.21 ± 0.13	0.39	28.3
weighted mean	0.26 ± 0.13	0.39	28.3
weighted mean with clipping	0.13 ± 0.10	0.30	21.8

^a in units of $10^{-17} \text{ ergs s}^{-1} \text{ cm}^{-2}$

^b in units of $10^{40} \text{ ergs s}^{-1}$

absorption trough before stacking. While this exercise makes our stacked spectrum insensitive to the presence of continuum light from the DLA galaxy, it will not affect the detectability of the Ly α line.

The flux in each pixel of the combined spectrum is calculated by averaging the fluxes of all spectra at this position. Arithmetic mean and weighted mean are both used. In the case of weighted mean the i-band signal-to-noise ratio (SNR) is used as the weighting factor for each spectrum. We calculate the uncertainty in each pixel of the combined spectrum as the standard deviation around the mean value. We obtain a third average spectrum from the weighted mean of the values in each pixel after rejecting the 5% extreme values on either positive and negative sides.

The stacked spectra obtained using simple mean, weighted mean, and weighted mean with clipping together with associated errors are shown in Fig. 1. We also show the stacked synthetic absorption DLA profiles in the corresponding samples as red continuous curves. The dashed blue curves are the synthetic profiles obtained using the lower and upper limits on $N(\text{H I})$ obtained in individual systems. To calculate the Ly α emission flux, in each stacked spectrum, we restrict ourselves to the wavelength range covered by the core of synthetic spectrum obtained from the lower limits on $N(\text{H I})$ (i.e inner dotted profiles in Fig. 1). We obtain the limit on the Ly α emission line flux by integrating the observed flux over a gaussian function with FWHM of 200 km s^{-1} . This value corresponds to the mean velocity widths of low ionization lines in DLAs (Ledoux et al. 2006) convolved with the SDSS instrumental broadening. The observed FWHM of the low ionization lines in our composite spectrum is consistent with this value.

The Ly α flux measurements are summarised in Table 1 and the gaussian fits are shown in the insets of Fig. 1. We do see marginal Ly α flux at the expected position at a $\leq 2\sigma$ level in the case of simple and weighted mean. In the case of clipped mean the bottom of the Ly α absorption profile is consistent with no Ly α emission. We estimate the 3σ upper limit ($F_{3\sigma}(\text{Ly}\alpha)$) given in Table 1) by using the gaussian fitting errors. As expected, the 3σ limit from the clipped mean is smaller than that from the other two methods. As this is the case with less contamination by outliers, we use the upper limit from the clipped mean composite spectrum, $F_{3\sigma}(\text{Ly}\alpha) < 3.0 \times 10^{-18} \text{ erg s}^{-1} \text{ cm}^{-2}$, for all further discussions. For the SDSS fibre diameter, 3 arcsec, this limit translates to a limiting 1σ surface brightness limit of $1.4 \times 10^{-19} \text{ ergs s}^{-1} \text{ cm}^{-2} \text{ arcsec}^{-2}$. This is only 1.7 times higher than that achieved in the very deep long slit spectroscopic observations by Rauch et al. (2008).

The flux limit we have achieved in the stacked spectrum is almost one order of magnitude smaller than the flux measured in the case of direct detections of Ly α emission from DLA galaxies (see Møller et al. 2004; Fynbo et al. 2010) and the typical flux limits reported for individual measurements (see Christensen et al. 2007). In addition the flux limit we have reached is much deeper than the one reached in typical blind narrow band searches for Ly α -

¹ The wavelength range affected by sky lines are 4040-4060 \AA , 4340-4380 \AA , 5170-5230 \AA , 5450-5475 \AA and $\geq 5560\text{\AA}$.

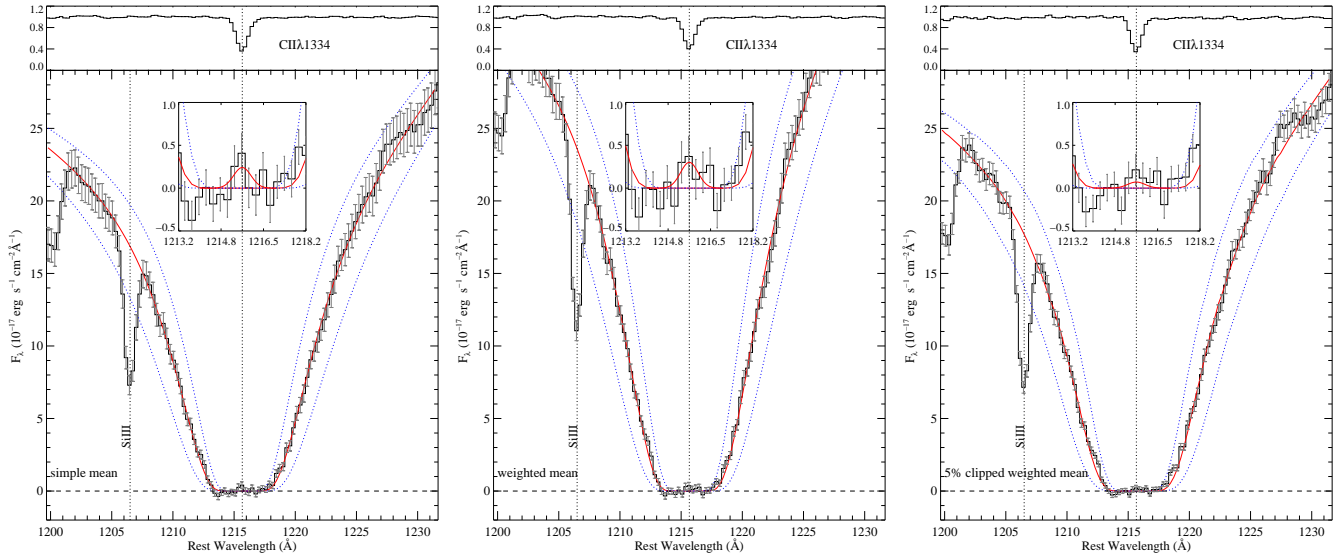


Figure 1. Stacked spectrum of DLAs obtained from simple mean, weighted mean, and weighted mean with 5% clipping are shown in, respectively, the left, middle and right panels. The red continuous curves are the stacked spectrum of the DLA synthetic absorption profiles. The dashed blue curves are the synthetic profiles obtained using the lower and upper limits on $N(\text{H I})$ as measured in each DLA. A gaussian with $FWHM = 200 \text{ km s}^{-1}$ is fitted in the bottom of the absorption trough and is shown by a red continuous curve in the inset. *Top panels:* profile of C II $\lambda 1334$ line to give an idea of the velocity spread of neutral gas.

emitters (see Ouchi et al. 2008) and comparable to the deepest limit achieved in the VVDS-LAE survey by Cassata et al. (2010).

For the mean redshift of our sample, $\langle z \rangle = 2.86$, our limiting flux corresponds to a Ly α luminosity of $2 \times 10^{41} \text{ erg s}^{-1}$ (see Table 1) or $\sim 0.03 L^* (\text{Ly}\alpha)$ if we use the Schechter function parameter $L^* = 5.8 \times 10^{42} \text{ erg s}^{-1}$ from the narrow band Ly α search by Ouchi et al. (2008). Thus it appears that on an average, DLAs at $z \sim 2.8$ trace the faint end luminosity of Ly α emitters.

4 STAR FORMATION

We estimate the average SFR in DLAs assuming that Ly α photons mainly originate from H II regions around massive stars and case B recombination (Osterbrock 1989). Then the Ly α luminosity is related to the SFR (\dot{M}_{SF}) by,

$$L_{\text{Ly}\alpha} = 0.68 h\nu_{\alpha} (1 - f_{\text{esc}}) N_{\gamma} \dot{M}_{\text{SF}}. \quad (1)$$

Here, $h\nu_{\alpha} = 10.2 \text{ eV}$ and f_{esc} are, respectively, the energy of a Lyman- α photon and the escape fraction of Lyman continuum photons. We use $f_{\text{esc}} \simeq 0.1$ as measured from stacked spectra of high- z LBGs (Shapley et al. 2006). Further, N_{γ} is the number of ionizing photons released per baryon of star formation. This is mainly a function of the metallicity and the stellar initial mass function (see Table 1 of Samui et al. 2007). As high redshift DLAs have generally low metallicities, $[Z/Z_{\odot}] \sim -1.5$ (see Fig 3 of Noterdaeme et al. 2008), we interpolate values of Table 1 of Samui et al. (2007) to have $N_{\gamma} = 9870$ corresponding to $[Z/Z_{\odot}] = -1.5$ and a Salpeter initial mass function with $\alpha = 2.35$. Ly α photons are sensitive to different kinds of radiation transport effects including resonant scattering (within the ISM as well as the intergalactic medium (IGM) and attenuation via dust. Hence, the observed Ly α luminosity can be related to the emitted luminosity by

$$L_{\text{Ly}\alpha}^{\text{obs}} = f_{\text{esc}}^{\text{Ly}\alpha} L_{\text{Ly}\alpha}, \quad (2)$$

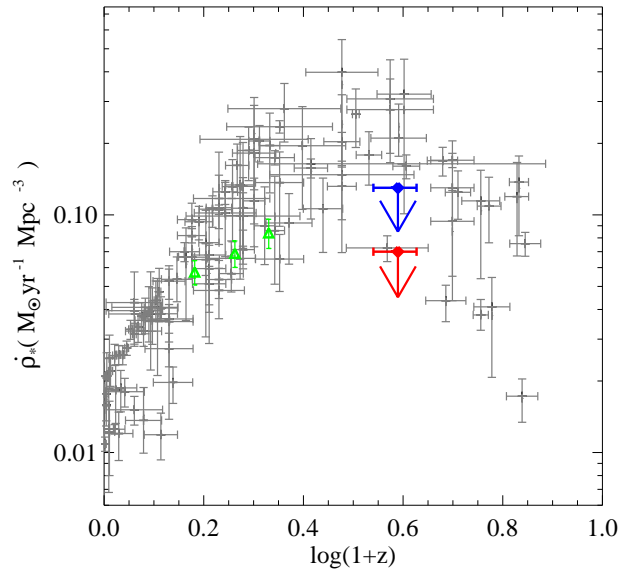


Figure 2. Evolution of the cosmic star formation rate density with redshift. The black points with error bars are taken from Hopkins & Beacom (2006). The red point refers to the 3σ upper limit on the contribution of DLA galaxies with $\log N(\text{H I}) \geq 20.62$ as measured in this work. The blue point is the same assuming all DLAs with $\log N(\text{H I}) \geq 20.30$ contribute the same. The green points show the contribution of Mg II systems estimated by Ménard et al. (2009).

where $f_{\text{esc}}^{\text{Ly}\alpha}$ is the escape probability of the Ly α photons. It is well known that only a small fraction of LBGs are Ly α emitters and even in these cases only a small fraction of Ly α photons escape the galaxy (see Kornei et al. 2010). Taking this fact into account it is appropriate to use a volumetric $f_{\text{esc}}^{\text{Ly}\alpha}$ of 0.05 as estimated by Hayes et al. (2010) for high- z galaxies. With these assumptions, the 3σ upper limit we have obtained above corresponds

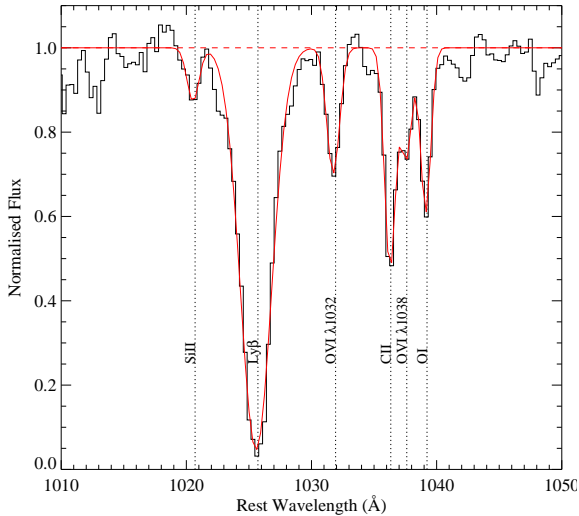


Figure 3. Wavelength range of the SDSS composite spectrum encompassing the O VI absorptions. Gaussian fits to some of the absorption lines are also overlotted

to a SFR of $\leq 1.2 M_{\odot} \text{ yr}^{-1}$. For comparison, this limiting value is higher than the average SFR of $0.1\text{--}0.5 M_{\odot} \text{ yr}^{-1}$ measured in low- z Mg II and Ca II systems (Wild et al. 2007; Noterdaeme et al. 2010; Ménard et al. 2009).

The SFR per unit comoving volume for DLAs is given by

$$\dot{\rho}_*(z) = \langle \dot{\psi}_*(z) \rangle (A/A_p) dN/dX \quad (3)$$

where $\langle \dot{\psi}_*(z) \rangle$ is the average SFR per unit physical area at z , A is the average physical cross-sectional area, A_p is the average projection of A on the plane of the sky, and dN/dX is the incidence of DLAs per unit absorption distance interval. We convert the star formation rate (\dot{M}_{SF}) to $\langle \dot{\psi}_*(z) \rangle$ by assuming the typical size of DLAs to be similar to that of faint Ly α emitters, $R = 10$ kpc.

We estimate dN/dX to be $9.95 \times 10^{-6} \text{ Mpc}^{-1}$ and $\dot{\rho}_* \leq 0.07 M_{\odot} \text{ yr}^{-1} \text{ Mpc}^{-3}$ for DLAs with $\log N(\text{H I}) \geq 20.62$ at $z = 2.86$ assuming $(A/A_p) = 2$. If we assume the upper limit on the Ly α flux is also valid for all DLAs with $\log N(\text{H I}) \geq 20.3$, then we get $\dot{\rho}_* \leq 0.13 M_{\odot} \text{ yr}^{-1} \text{ Mpc}^{-3}$. It is to be remembered that increasing R or $f_{\text{esc}}^{\text{Ly}\alpha}$ will further decrease $\dot{\rho}_*$. In Fig. 2 we compare these values with the extinction corrected comoving star formation rate density measurements summarized in Hopkins & Beacom (2006). The conservative upper limits from our study are comparatively lower than the measurements based on LBGs.

5 HIGH-IONIZATION GAS PROBED BY O VI ABSORPTION

If DLAs are associated with star forming regions, they should be associated with hot gas related to galactic outflows and/or infall of primordial gas. Indeed, numerical simulations of cosmological structure formation (e.g Davé et al. 2001) predict that gas falling onto diffuse large-scale structures will be accelerated to supersonic speeds and become shock-heated to temperatures of 10^5 to 10^7 K, creating a phase known as the warm-hot IGM. Similarly a sustained star formation activity in galaxies can lead to super novae driven outflows of hot gas. Observations of high- z Lyman Break Galaxies (LBGs) frequently show galactic scale superwinds and the mass

outflow rate may be intimately related to the star formation rate (Pettini et al. 2001). This hot gas can be traced by O VI absorption.

Fox et al. (2007) have detected O VI in at least 34% of the DLAs and suggested that O VI could be present in 100% of them. We confirm this finding by detecting the O VI doublet (with rest equivalent width $W_r(\text{O VI } \lambda 1032) = 0.4 \text{ \AA}$) in our composite spectrum (see Fig. 3). The average deconvolved velocity width of the O VI lines ($\sim 275 \text{ km s}^{-1}$) is systematically higher than that of C IV ($\sim 250 \text{ km s}^{-1}$), Si IV ($\sim 205 \text{ km s}^{-1}$) and singly ionization lines ($\sim 120 \text{ km s}^{-1}$). The velocity range spanned by the hot phase is therefore a factor of two larger than that of the neutral phase. This suggests a connection between actively star forming regions with outflowing and/or infalling hot gas and DLAs.

6 SUMMARY AND DISCUSSION

Using a sample of 341 DLAs with $\log N(\text{H I}) \geq 20.62$ we place a 3σ upper limit of $3.0 \times 10^{-18} \text{ erg s}^{-1} \text{ cm}^{-2}$ on the Ly α flux emitted at the redshift of the DLA within ~ 1.5 arcsec (or 12 kpc at $z \sim 2.86$) to the QSO line-of-sight. This corresponds to an average Ly α luminosity of $\leq 2 \times 10^{41} \text{ erg s}^{-1}$ or an object with a luminosity of $0.03 L_{\star}(\text{Ly}\alpha)$. Thus, the typical DLA population seems to originate from the low luminosity end of the high redshift Ly α emitting galaxies.

At low redshift the star forming galaxies obey the Kennicutt & Schmidt law,

$$\begin{aligned} \langle \dot{\psi}_{\star} \rangle_{\perp} &= 0 \text{ when } N_{\perp} < N_{\perp}^{\text{crit}} \\ &= K(N_{\perp}/N_{\perp}^{\text{c}})^{\beta}, \quad N_{\perp} \geq N_{\perp}^{\text{crit}}. \end{aligned} \quad (4)$$

Kennicutt (1998a,b) have found $K = (2.5 \pm 0.5) \times 10^{-4} M_{\odot} \text{ yr}^{-1} \text{ kpc}^{-2}$, $\beta = 1.4 \pm 0.15$, $N_{\perp}^{\text{c}} = 1.25 \times 10^{20} \text{ cm}^{-2}$ and $\log N_{\perp}^{\text{crit}} = 20.62$. Using the above equation and the $N(\text{H I})$ distribution of our sample we would expect to measure in our experiment a surface SFR of $5.5 \times 10^{-3} M_{\odot} \text{ yr}^{-1} \text{ kpc}^{-2}$. Assuming DLAs have a radius of 10 kpc gives an expectation of $1.7 \pm 0.4 M_{\odot} \text{ yr}^{-1}$. This is higher than our $1.2 M_{\odot} \text{ yr}^{-1}$ 3σ upper limit derived in the previous Section. This suggests that star formation in DLAs is less efficient compared to what is seen in the H I disks of nearby galaxies. This is consistent with the conclusions by Wolfe & Chen (2006). In the local universe such low star formation efficiencies are seen either in the outer regions of galaxies or in dwarf galaxies (Roychowdhury et al. 2009; Bigiel et al. 2010).

Using C II* absorption lines, Wolfe et al. (2003a) have estimated the SFR per unit area, $\langle \dot{\psi}_{\star} \rangle = 10^{-2.19}$ and $10^{-1.32} M_{\odot} \text{ yr}^{-1} \text{ kpc}^{-2}$ for CNM (cold neutral medium) and WNM (warm neutral medium) models, respectively. The pure WNM solution will require an unphysically low escape fraction (≤ 0.004) of Ly α photons in order for the model to comply with our upper limit. As DLAs have very little dust content, such low Ly α escape fraction is unlikely. In the case of the CNM solution, for the upper limit we observe to be consistent with the C II* measurements, the Ly α escape fraction $f_{\text{esc}}^{\text{Ly}\alpha}$ should be smaller than 0.03. This value, although low, is similar to that estimated in LBGs (Hayes et al. 2010). Note that the high-cool population of C II* as defined by Wolfe et al. (2008) will also require unphysically low values of $f_{\text{esc}}^{\text{Ly}\alpha}$. In any case, it can be concluded that in situ star formation is low in DLAs.

Using deep long-slit spectroscopy of an empty field, Rauch et al. (2008) have detected extended and weak Ly α emitters at $2.67 \leq z \leq 3.75$. Based on the projected size (a median radius of $0.99''$ corresponding to a physical size of 7.7 kpc) and a volume density of $3 \times 10^{-2} h_{70}^3 \text{ Mpc}^{-3}$, they found that the number per unit redshift of these emitters is consistent with that of DLAs. The

individual Ly α flux in these objects range from 1.5 to 15 $\times 10^{-18}$ erg s $^{-1}$ cm $^{-2}$ with mean and median fluxes of, respectively, 3.7 and 3 $\times 10^{-18}$ erg s $^{-1}$ cm $^{-2}$. If typical DLAs were associated with these objects (with sizes less than the projected size of the SDSS fibre), then we should have detected Ly α emission in the stacked spectrum. Thus the analysis presented here does not support the idea that the unresolved or centrally dominated faint Ly α emitters found by Rauch et al. (2008) are the host-galaxies of DLAs with $\log N(\text{H I}) \geq 20.62$. However, our analysis can not rule out DLAs being similar to their amorphous extended class of objects with sizes ≥ 10 kpc.

In summary, there are strong evidences for DLAs to be associated with regions of star-formation: (i) the median metallicity of DLAs is of the order of $10^{-1.5}$ solar (Noterdaeme et al. 2008) and is always larger than 10^{-3} solar (Penprase et al. 2010); (ii) we confirm the findings by Fox et al. (2007) that strong O VI absorption is associated with DLAs with a velocity spread (FWHM ~ 250 km s $^{-1}$) about twice larger than the velocity spread of the low-ionization gas suggesting bulk-motions in the hot phase due to kinematical input from supernovae and/or gravitational effects; (iii) C II* is detected in almost half of the DLAs and can only be explained by energy input from star-formation activity (Wolfe et al. 2008). However, we show here that the mean Ly α emission within 12 kpc from DLAs is smaller than the emission in most of the weak Ly α emitters detected by Rauch et al. (2008) and is consistent with very low in situ star formation rates. Therefore, the DLA phase could be spread far away from the center of the star forming regions. The hot phase associated with DLAs could then be the relics of past wind episodes in the star forming regions.

ACKNOWLEDGEMENT

We acknowledge the use of SDSS spectra from the archive (<http://www.sdss.org/>). RS and PPJ gratefully acknowledge the support from the IFCPAR. PN is supported by a CONICYT/CNRS fellowship.

REFERENCES

- Bigiel, F., Leroy, A., Walter, F., Blitz, L., Brinks, E., de Blok, W. J. G., & Madore, B., 2010, ArXiv e-prints
- Bunker, A. J., Warren, S. J., Clements, D. L., Williger, G. M., & Hewett, P. C., 1999, MNRAS, 309, 875
- Burbidge, E. M., Beaver, E. A., Cohen, R. D., Junkkarinen, V. T., & Lyons, R. W., 1996, AJ, 112, 2533
- Cassata, P., Le Fèvre, O., Garilli, B., et al., 2010, ArXiv e-prints
- Christensen, L., Wisotzki, L., Roth, M. M., Sánchez, S. F., Kelz, A., & Jahnke, K., 2007, A&A, 468, 587
- Colbert, J. W. & Malkan, M. A., 2002, ApJ, 566, 51
- Davé, R., Cen, R., Ostriker, J. P., et al., 2001, ApJ, 552, 473
- Fox, A. J., Petitjean, P., Ledoux, C., & Srianand, R., 2007, A&A, 465, 171
- Fynbo, J. P. U., Laursen, P., Ledoux, C., et al., 2010, ArXiv e-prints
- Hayes, M., Östlin, G., Schaerer, D., et al., 2010, Nature, 464, 562
- Heinmüller, J., Petitjean, P., Ledoux, C., Caucci, S., & Srianand, R., 2006, A&A, 449, 33
- Hirashita, H. & Ferrara, A., 2005, MNRAS, 356, 1529
- Hopkins, A. M. & Beacom, J. F., 2006, ApJ, 651, 142
- Kennicutt, Jr., R. C., 1998a, ARA&A, 36, 189
- , 1998b, ApJ, 498, 541
- Kornei, K. A., Shapley, A. E., Erb, D. K., Steidel, C. C., Reddy, N. A., Pettini, M., & Bogosavljević, M., 2010, ApJ, 711, 693
- Kulkarni, V. P., Woodgate, B. E., York, D. G., Thatte, D. G., Meiring, J., Palunas, P., & Wassell, E., 2006, ApJ, 636, 30
- Le Brun, V., Bergeron, J., Boissé, P., & Deharveng, J. M., 1997, A&A, 321, 733
- Ledoux, C., Petitjean, P., Fynbo, J. P. U., Møller, P., & Srianand, R., 2006, A&A, 457, 71
- Ledoux, C., Petitjean, P., & Srianand, R., 2003, MNRAS, 346, 209
- Lehner, N., Wakker, B. P., & Savage, B. D., 2004, ApJ, 615, 767
- Lowenthal, J. D., Hogan, C. J., Green, R. F., Woodgate, B., Caulet, A., Brown, L., & Bechtold, J., 1995, ApJ, 451, 484
- Ménard, B., Wild, V., Nestor, D., Quider, A., & Zibetti, S., 2009, ArXiv:0912.3263
- Møller, P., Fynbo, J. P. U., & Fall, S. M., 2004, A&A, 422, L33
- Møller, P., Warren, S. J., Fall, S. M., Fynbo, J. U., & Jakobsen, P., 2002, ApJ, 574, 51
- Moller, P., Warren, S. J., & Fynbo, J. U., 1998, A&A, 330, 19
- Noterdaeme, P., Ledoux, C., Petitjean, P., & Srianand, R., 2008, A&A, 481, 327
- Noterdaeme, P., Petitjean, P., Ledoux, C., & Srianand, R., 2009, A&A, 505, 1087
- Noterdaeme, P., Petitjean, P., Srianand, R., Ledoux, C., & Le Petit, F., 2007, A&A, 469, 425
- Noterdaeme, P., Srianand, R., & Mohan, V., 2010, MNRAS, 403, 906
- Osterbrock, D. E., 1989, Astrophysics of Gaseous Nebulae and Active Galactic Nuclei (Mill Valley: University Science Books)
- Ouchi, M., Shimasaku, K., Akiyama, M., et al., 2008, ApJS, 176, 301
- Penprase, B. E., Prochaska, J. X., Sargent, W. L. W., Toro Martinez, I., & Beeler, D. J., 2010, ArXiv:1006.4119
- Petitjean, P., Srianand, R., & Ledoux, C., 2000, A&A, 364, L26
- Pettini, M., Shapley, A. E., Steidel, C. C., Cuby, J., Dickinson, M., Moorwood, A. F. M., Adelberger, K. L., & Giavalisco, M., 2001, ApJ, 554, 981
- Prochaska, J. X. & Wolfe, A. M., 2009, ApJ, 696, 1543
- Rao, S. M., Nestor, D. B., Turnshek, D. A., Lane, W. M., Monier, E. M., & Bergeron, J., 2003, ApJ, 595, 94
- Rauch, M., Haehnelt, M., Bunker, A., et al., 2008, ApJ, 681, 856
- Roychowdhury, S., Chengalur, J. N., Begum, A., & Karachentsev, I. D., 2009, MNRAS, 397, 1435
- Samui, S., Srianand, R., & Subramanian, K., 2007, MNRAS, 377, 285
- Shapley, A. E., Steidel, C. C., Pettini, M., Adelberger, K. L., & Erb, D. K., 2006, ApJ, 651, 688
- Srianand, R., Petitjean, P., Ledoux, C., Ferland, G., & Shaw, G., 2005, MNRAS, 362, 549
- Warren, S. J. & Moller, P., 1996, A&A, 311, 25
- Wild, V., Hewett, P. C., & Pettini, M., 2007, MNRAS, 374, 292
- Wolfe, A. M. & Chen, H., 2006, ApJ, 652, 981
- Wolfe, A. M., Gawiser, E., & Prochaska, J. X., 2003a, ApJ, 593, 235
- Wolfe, A. M., Prochaska, J. X., & Gawiser, E., 2003b, ApJ, 593, 215
- Wolfe, A. M., Prochaska, J. X., Jorgenson, R. A., & Rafelski, M., 2008, ApJ, 681, 881